

## Observation of Electronic Spectra of Three Isomers of 2,6-Difluoropyridine–Water Clusters

Yoshinori Nibu,\* Chie Okabe,† and Hiroko Shimada

Department of Chemistry, Faculty of Science, Fukuoka University, Nanakuma 8-19-1 Jonann-ku, Fukuoka 814-0180, Japan

Received: August 19, 2002; In Final Form: January 7, 2003

Electronic spectra of bare and hydrogen-bonded clusters of 2,6-difluoropyridine with water were observed in a supersonic free jet. The spectra indicate the existence of three isomers for 2,6-difluoropyridine–H<sub>2</sub>O 1:1 clusters. Ab initio molecular orbital calculations also support this result. The structures of the three clusters have hydrogen bonding between water hydrogen and nitrogen (N-site), water hydrogen and fluorine (F-site), and water oxygen and aromatic hydrogen (H-site). In the ground states of cluster cations, calculations suggest the existence of H-site cluster structure, and experiments also support these results. Following excitation into the D<sub>0</sub> state of the N-site cluster from the S<sub>1</sub> state, the cluster dissociates into bare 2,6-difluoropyridine and water, and the molecular orbital calculation also supports this result.

## 1. Introduction

Hydrogen bonding is the most important intermolecular interaction, and the study of hydrogen-bonded clusters in supersonic free jets gives important information about this interaction from a microscopic point of view. The cluster formation of water molecules is especially important to the understanding of the hydrogen bond effect that plays an important role in the chemical or biological phenomenon. The derivatives of pyridine exist widely in biological systems, and understanding hydrogen bonding with water is not only a chemically but also a biologically important issue. Despite the simplicity of the molecule, there have been quite a few studies of the electronic spectrum of pyridine in supersonic free jets<sup>1,2</sup> since pyridine is one of the most famous nonfluorescent molecules. Accordingly, the electronic spectrum of hydrogen-bonded pyridine in jets has not been reported yet. However, some pyridine derivatives give fluorescence from the electronic excited state, and the hydrogen-bonding clusters were observed in a supersonic free jet.<sup>3</sup>

We found out that the fluorine substitution of pyridine gives fluorescence from the electronic excited state. Fluorine-substituted pyridine is expected to form hydrogen bonds with water through the nitrogen atom in the pyridine ring. This type of hydrogen bonding, where the nitrogen atom of the heteroaromatic ring behaves as a proton acceptor, is familiar in biological systems.

For hydrogen-bonded clusters, the electronic transitions of phenol clusters have been extensively studied by many workers.<sup>4</sup> In 1:1 phenol–water clusters, the phenol molecule behaves as a proton donor. The water molecule behaves as either a proton donor or a proton acceptor depending on the hydrogen-bonding partner. Therefore, the study of hydrogen-bonded clusters where the water molecule behaves as a proton donor is also interesting. The aza-aromatic compound is expected to behave as a proton acceptor when hydrogen bonds are formed with water molecules. Zewail and co-workers have reported on the hydrogen-bonding

effect of water on the S<sub>2</sub> state of isoquinoline.<sup>5,6</sup> They reported that the three peaks around the S<sub>2</sub> electronic origin become a single peak because the stabilization of the nonbonding orbital by hydrogen bonding reduces the interaction between S<sub>2</sub> ( $\pi$ ,  $\pi^*$ ) and lower-lying S<sub>1</sub> ( $n$ ,  $\pi^*$ ) states. Later, Bernstein et al. observed REMPI spectra of the clusters and discussed them for the structure of the clusters.<sup>7</sup> Wallace et al. also observed the electronic spectra of hydrogen-bonded 2-aminopyridine molecule.<sup>3</sup> Recently, Ohshima et al. observed the electronic and IR spectra of hydrogen-bonded acridine–water clusters in a jet and determined the structure based on the molecular orbital calculations.<sup>8</sup>

Clusters of water with various molecules have been reported. Hydrogen bond interactions with aromatic compounds are very interesting from the point of view of hydrogen– $\pi$  interactions. Brutschy and co-workers observed the IR spectra of the clusters of water with fluorine-substituted benzene in a supersonic free jet.<sup>9</sup> They suggested the structure having water hydrogen bonded to the  $\pi$ -electron cloud of the aromatic ring from the observed frequencies of the OH stretching vibrations of hydrogen-bonded water. Brenner et al. have observed the rotational contour of the electronic spectrum for the *p*-difluorobenzene–water 1:1 cluster and have performed theoretical calculation to obtain the stable structure.<sup>10</sup> They concluded that the oxygen and hydrogen atoms in water bond to the hydrogen and fluorine atoms in *p*-difluorobenzene, respectively. Tarakeshwar et al. performed MP2-level ab initio molecular orbital calculation with various basis functions and concluded that the most stable structure of water–fluorobenzene and water–*p*-difluorobenzene has a  $\sigma$ -type hydrogen bond (i.e., a water hydrogen bonds to fluorine and a water oxygen bonds to aromatic hydrogen<sup>11</sup>). They also have shown that the structure explains the observed IR frequencies of the OH stretching mode for hydrogen-bonded water well.

In this paper, the structure and dynamics of three isomers of DFP–water 1:1 clusters are discussed on the basis of the results of fluorescence excitation and dispersed fluorescence spectra, mass-resolved multiphoton ionization spectrum, and ab initio molecular orbital calculation. From the comparison of the experiment with the calculations, the structures of fluoroaromatics hydrogen bonded to water are also discussed.

\* Corresponding author. E-mail: nibu@cis.fukuoka-u.ac.jp.

† Present address: Department of Chemistry and Graduate School of Molecular Chemistry, Faculty of Science, Kyushu University, 6-10-1 Hakozaki, Higashi-ku, 812-8581 Fukuoka, Japan.

## 2. Methods

**2.1. Molecular Orbital Calculations.** Molecular orbital calculations for DFP–water clusters were performed with the Gaussian 98 program<sup>12</sup> at the Information Technology Center of Fukuoka University. The structure optimization and frequency calculations for the  $S_0$  states of DFP–water clusters were carried out with B3LYP/6-31G\*\*, B3LYP/6-311++G\*\*, MP2/6-31G\*\*, and MP2/6-311++G\*\*. First, various structures, which were referred to those obtained for the clusters of benzene,<sup>13</sup> fluorobenzene,<sup>11</sup> *p*-difluorobenzene,<sup>11</sup> and pyridine<sup>14</sup> with water, were selected as initial structures to carry out B3LYP/6-31G\*\* calculations. The optimized structures obtained above were used as initial structures for B3LYP/6-311++G\*\*, MP2/6-31G\*\*, and MP2/6-311++G\*\* calculations. In the latter three calculations,  $\pi$ -bonded structures obtained for fluorobenzene–water and *p*-difluorobenzene–water clusters<sup>11</sup> were also used as initial structures. The obtained energies were corrected for basis set superposition error (BSSE)<sup>15</sup> and zero-point vibration. The vibrational frequencies of DFP–D<sub>2</sub>O cluster were also calculated. For the  $D_0$  state, optimization and vibrational frequency calculations were carried out with B3LYP/6-31G\*\* and B3LYP/6-311++G\*\*, and no MP2 calculation could be performed because MP2 calculations were too heavy.

**2.2. Experimental.** DFP–water clusters were formed and cooled in a pulsed supersonic expansion using He carrier gas with 5 atm of backing pressure. DFP and water were mixed in a nozzle housing and expanded into a vacuum chamber. The apparatus of the supersonic free jet and the setup for the observation of the fluorescence excitation spectrum have been reported elsewhere.<sup>16</sup> Hole-burning spectra detected with laser-induced fluorescence were observed using two dye laser systems that are shown as follows. A PDL-II (Spectra Physics) excited by a DCR-11 Nd:YAG laser (Spectra Physics) was used as a probe laser, and an FL2005 (Laser Analytic Systems) excited by a GCR-130 Nd:YAG laser (Spectra Physics) was used as a pump laser. The time interval between the lasers was set to 500 ns.

For the observation of the multiphoton ionization spectrum, the ion generated by photoionization was detected with an electron multiplier, Ceratron (Murata Co. Ltd.), that was placed at 5 cm from the ionization point. In the experimental setup, the arrival time of the ions due to the different masses was measured. The resolution of the apparatus was enough to resolve the peaks due to bare DFP and hydrogen-bonded DFP with water. For the two-color ionization experiment, the two dye lasers, mentioned above, were used without a time delay.

The laser-induced fluorescence was dispersed with a Spex 1702 spectrometer equipped with an image-intensified charge-coupled device (ICCD) detector (Princeton Instruments ITE-1024M). The wavelength of the ICCD detector was calibrated with a Ne lamp, and the reproducibility of the peak position was less than 0.5 cm<sup>-1</sup>. The total resolution of the system, which is determined from the slit width of the monochromator and the spatial resolution of the ICCD detector, was estimated to be about 5 cm<sup>-1</sup> fwhm throughout the experiments. Dispersed fluorescence was accumulated on the ICCD for 100 s.

DFP was purchased from Aldrich Co Ltd. and was used without further purification. Deuterium oxide, obtained from CND Isotopes Ltd., was also used to observe frequency shifts of DFP–D<sub>2</sub>O clusters.

## 3. Results and Discussion

**3.1. Molecular Orbital Calculations.** The structures optimized with B3LYP/6-311++G\*\* calculations are shown in

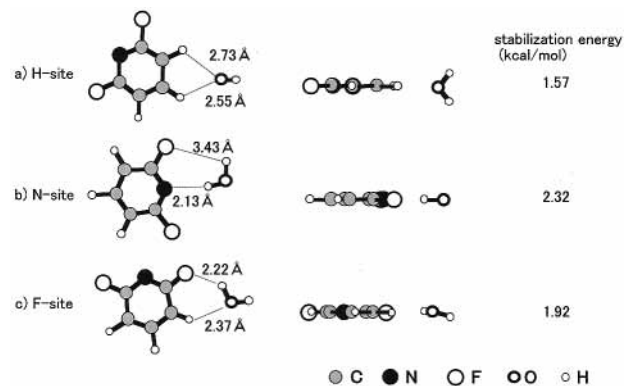


**Figure 1.** Optimized cluster structures and stabilization energies obtained with B3LYP/6-311++G\*\* for (a) H-site, (b) N-site, and (c) F-site clusters in the  $S_0$  state. The energies are corrected with BSSE and the zero-point vibrational energy.

**TABLE 1: Hydrogen Bond Energies for the Clusters (kcal/mol)**

method	B3LYP					
	6-31G**		6-311++G**			
basis set	H-site	N-site	F-site	H-site	N-site	F-site
species	H-site	N-site	F-site	H-site	N-site	F-site
stabilization energy	3.96	5.37	5.96	2.94	4.21	3.54
zero-point corrected	3.08	3.98	4.28	2.00	2.77	2.28
BSSE corrected	2.15	3.24	2.43	2.51	3.77	3.18
BSSE + zero point	1.27	1.86	0.75	1.57	2.32	1.92
method	MP2					
	6-31G**		6-311++G**			
basis set	H-site	N-site	F-site	H-site	N-site	F-site
species	H-site	N-site	F-site	H-site	N-site	F-site
stabilization energy	4.34	5.95	6.25	4.25	5.10	4.72
zero-point corrected	3.45	4.56	4.64	3.08	3.77	3.36
BSSE corrected	2.68	3.47	2.66	2.84	3.84	3.35
BSSE + zero point	1.80	2.08	1.06	1.67	2.50	1.99

Figure 1. Stabilization energies obtained with various calculation methods are also shown in Table 1. As shown in Figure 1, the three clusters are called H-site (Figure 1a), N-site (Figure 1b), and F-site (Figure 1c) clusters hereafter. Structures other than these three were not obtained within our calculations, in which various initial structures and calculation methods were tried to obtain structural isomers. It is interesting that Brenner et al. have also reported H-site and F-site structures for *p*-difluorobenzene–water 1:1 clusters, where a different method was used to obtain a stable cluster structure.<sup>10</sup> They have also suggested the possibility of the  $\pi$ -bonded structure, where a water molecule in the cluster bonds to the  $\pi$  electrons of *p*-difluorobenzene. However, no  $\pi$ -bonded structure was obtained for the DFP–water 1:1 cluster within our calculations. As seen from Table 1, BSSE + zero-point energy corrected values give surprisingly similar results both in the B3LYP/6-311++G\*\* and MP2/6-311++G\*\* calculations. From the calculations with the basis set of 6-311++G\*\*, it is concluded that the N-site cluster is the most stable structure for BSSE + zero-point energy corrected values among the three clusters.

For H-site, N-site, and F-site clusters, the water molecule mainly interacts with two hydrogen atoms, the nitrogen atom, and a fluorine atom of the DFP molecule, respectively.

The structure of the N-site cluster is expected for the hydrogen-bonding form between water and pyridine,<sup>14</sup> where pyridine behaves as a proton-accepting molecule through the lone-pair electrons of the nitrogen atom in the pyridine ring. The calculated bond distance between hydrogen and nitrogen

is 2.13 Å for the N-site cluster. From the calculation of clusters between fluoropyridines and water by B3LYP/6-311++G\*\*, where a water hydrogen mainly interacts with the nitrogen atom of the pyridine ring, the N–H distances are 1.94, 2.00, and 2.18 Å for the pyridine–water, 2-fluoropyridine–water, and 2,3,5,6-tetrafluoropyridine–water clusters, respectively. The comparison of the hydrogen bond distances shows that the hydrogen bond of the N-site cluster of the DFP–water cluster is weaker than that of pyridine–water and 2-fluoropyridine–water clusters and stronger than that of 2,3,5,6-tetrafluoropyridine. Because the N–H bond distance of the clusters strongly depends on the number of substituted fluorines, it is concluded that fluorine substitution decreases the hydrogen-bonding ability of the nitrogen atom in the pyridine ring.

In the H-site cluster, the oxygen atom of the water molecule bonds to hydrogen atoms in the pyridine ring. The distances between the hydrogen atoms of DFP and the oxygen atom of water are 2.73 and 2.55 Å, respectively.

The F-site cluster has two hydrogen-bonding interactions between a hydrogen atom of water and a fluorine atom of DFP and between the oxygen of water and a hydrogen atom of DFP. The structure is similar to that suggested by Tarakeshwar et al. by higher-level *ab initio* molecular orbital calculations for fluorobenzene–water and *p*-difluorobenzene–water clusters.<sup>11</sup>

The stabilization energies with the zero-point energy and BSSE corrections of the clusters are 1.57, 2.32, and 1.92 kcal/mol for H-site, N-site, and F-site clusters, respectively, as shown in Table 1. These values indicate that the three clusters have similar stabilization energies despite the differences in the structures. The similarity of the stabilization energy could cause the appearance of the three types of DFP–water clusters in a supersonic free jet, which will be discussed in a latter section.

MP2 calculations also have been made with basis sets of 6-31G\*\* and 6-311++G\*\* for the three clusters. As a result, the three optimized structures coincide with the structures from B3LYP/6-31G\*\* calculations except for small structural differences. Despite various calculations with many initial structures including  $\pi$ -bonded structures and basis sets, the cluster structure of hydrogen bonding to  $\pi$  electrons, which was obtained for benzene–water clusters, was not obtained for DFP–water in the electronic ground state. It has been pointed out that the density functional method is not appropriate for predicting the structure and bond energies of weakly bound van der Waals clusters such as the benzene–water cluster.<sup>11</sup> However, because the calculations of DFP–water clusters give consistent results between the DFT method of the B3LYP functional and the MP2 method with the 6-311++G\*\* basis set, as shown in Table 1, the calculation with the B3LYP functional is applicable to DFP–water clusters, which have relatively stronger hydrogen bonding than benzene–water clusters. Therefore, from the results of molecular orbital calculations, it is concluded that the DFP–water 1:1 cluster has three conformational isomers in the ground state. This fact corresponds well to the experimental results in the fluorescence excitation spectra of DFP–water clusters.

The stable structures in the cationic  $D_0$  state of the clusters were also calculated with the B3LYP/6-311++G\*\* method with the optimized structures obtained in the  $S_0$  states as initial structures. In the calculations, two types of structures were obtained, as shown in Figure 2. One of the two structures corresponds to the H-site cluster obtained for the  $S_0$  state. Another structure, where the oxygen atom of water bonds to the  $\pi$  cloud of DFP, is also stable. The latter structure was obtained only in the  $D_0$  state. The  $\pi$ -bonded structure for the

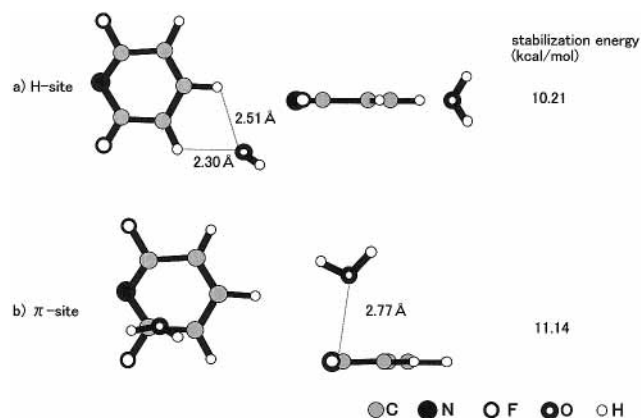


**Figure 2.** Optimized cluster structures and stabilization energies in the  $D_0$  states with B3LYP/6-311++G\*\*. The stabilization energies are corrected for the zero vibrational level.

$S_0$  state could not be obtained even though the  $\pi$ -bonded structure obtained for the  $D_0$  state was used as an initial structure for the optimization. As a result, two stable structures are expected in the  $D_0$  state of the DFP–water 1:1 cluster from the results of B3LYP/6-311++G\*\* calculations. It is interesting that a similar structure was also observed for the benzene<sup>+</sup>–water cluster.<sup>13b,c</sup>

The stable structures of N-site and F-site clusters in the  $D_0$  state could not be obtained with the B3LYP/6-311++G\*\* calculations. A single-point energy calculation in the  $D_0$  state for the N-site structure obtained in the  $S_0$  state gives a higher energy than the sum of the energies of bare DFP<sup>+</sup> and water. The phenomenon will be discussed later with the results of multiphoton ionization experiments.

Because pyridine behaves as a proton-accepting molecule, DFP, a fluorine derivative of pyridine, is also expected to behave as a proton acceptor through the nitrogen atom in the pyridine ring. The results of molecular orbital calculations show that the N-site cluster, where DFP behaves as a proton acceptor through nitrogen, has the largest stabilization energy among the three clusters in the  $S_0$  state.

**3.2. Fluorescence Excitation and Dispersed Fluorescence Spectra of Bare 2,6-Difluoropyridine.** Figure 3a shows the fluorescence excitation spectrum of bare DFP in a supersonic free jet expanded with He gas. As seen from the Figure, the band origin is located at 37 820  $\text{cm}^{-1}$  and coincides with the values reported previously by Mehdi, which were obtained with a UV absorption spectrum in the vapor phase.<sup>17</sup> Mehdi et al. assigned the  $S_1$  state to be a  ${}^1B_2(\pi, \pi^*)$  state. The reversal of the energy between the  $(\pi, \pi^*)$  and  $(n, \pi^*)$  states compared with those of pyridine is due to fluorine substitution because the substitution increases the energy of  $(n, \pi^*)$  states.<sup>18</sup>

The SVL spectrum from the band origin is shown in Figure 3b. The vibronic bands in the SVL spectrum could be assigned to totally symmetric vibrations from the results of infrared and Raman spectra,<sup>19</sup> except for the band at 487  $\text{cm}^{-1}$ . The SVL spectrum from the 0 + 142  $\text{cm}^{-1}$  band shows the progression with the frequency of 487  $\text{cm}^{-1}$ . This fact indicates that the frequency of 142  $\text{cm}^{-1}$  in the  $S_1$  state corresponds to 487  $\text{cm}^{-1}$  in the  $S_0$  state. In IR, far-IR, and Raman spectra of DFP in the liquid phase, no band was observed around 487  $\text{cm}^{-1}$ ; however, a band at 250  $\text{cm}^{-1}$  was observed. This band should be assigned to be a nontotally symmetric vibration from the depolarization experiment in the Raman spectra in the liquid phase. These results indicate that the 487  $\text{cm}^{-1}$  band could not be assigned to a fundamental vibration but to an overtone of a non-totally

**TABLE 2: Observed and Calculated Frequency Shifts of the Intramolecular Vibrations of DFP Due to Cluster Formation with Water<sup>a</sup>**

assignment	bare <sup>b</sup>			frequency shift/cm <sup>-1</sup> ( $\nu_{\text{cluster}} - \nu_{\text{bare}}$ ) <sup>c</sup>								
	calcd		obsd	H-site (A)			N-site (B)			F-site (C)		
	B3LYP	MP2		calcd	obsd	calcd		obsd	calcd		obsd	
$\nu_{9a}$	350	350	350	0		0	3		4	2		4
$2\nu_{11}$	488	489	487	8	6	26	4	0	-2	6	3	0
$\nu_{6a}$	551	547	546	-1	0	5	5	6	6	-1	1	-2
$\nu_1$	749	746	741	-2	-1	1	1	1	1	-3	-2	-3
$\nu_{12}$	1012	1014	998	-1	0	6	4	6	6	1	1	-1

<sup>a</sup> Vibrational frequencies were calculated with B3LYP/6-311G++G\*\* and MP2/6-311++G\*\* without scaling factor. <sup>b</sup> Observed and calculated frequencies for bare DFP. <sup>c</sup> Numbers indicate frequency shifts of intramolecular vibrations of DFP in the clusters from those in the bare DFP.

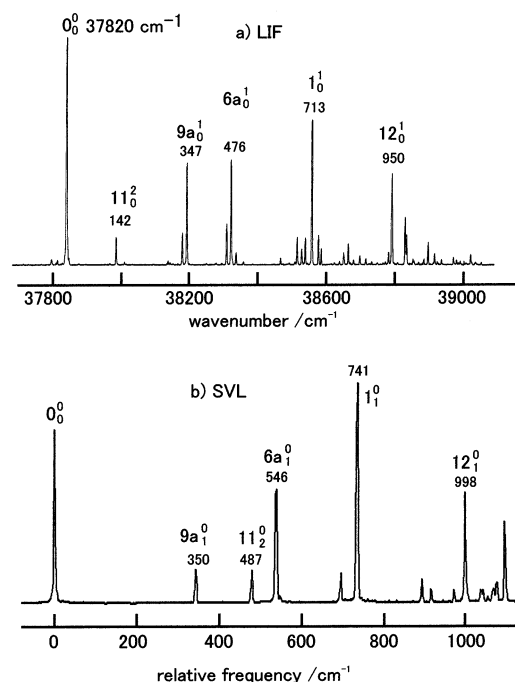


**Figure 3.** (a) Fluorescence excitation spectrum of bare DFP in a supersonic free jet. (b) Dispersed fluorescence spectrum from the band origin of bare DFP observed in a supersonic free jet.

symmetric vibration. Considering the frequency, the favorable candidate of the band is the overtone of  $\nu_{11}$ , an out-of plane vibration of fluorine atoms. The vibrational modes discussed in this study were based on the Wilson notation.<sup>20</sup> The calculated frequency of the  $\nu_{11}$  vibration is  $244 \text{ cm}^{-1}$ , with an ab initio calculation of B3LYP/6-311++G\*\*. (See Table 2.) The intensity distribution of the vibronic bands in the electronic spectra means that the molecular structure of DFP in the excited state has changed along the vibrational mode that appeared in the spectra. In the electronic transition to  $S_1(n, \pi^*)$  observed for pyridine or pyrazine, non-totally symmetric out-of-plane vibrations appear in the electronic transition because these vibrations effectively induce coupling between the  $S_1(n, \pi^*)$  and the higher-lying  $(\pi, \pi^*)$  states. The appearance of the non-totally symmetric vibrations is due to the intensity borrowing from the  $(\pi, \pi^*)$  state through vibronic coupling. If  $S_1$  is a  $(\pi, \pi^*)$  state, which usually has a higher transition probability than the  $(n, \pi^*)$  state does, vibronic coupling with the higher-lying  $(n, \pi^*)$  state, which has a weaker transition probability from the ground state, does not contribute to the intensity borrowing. However, because a vibronic interaction distorts the potential surface of the  $S_1(\pi, \pi^*)$  state along the non-totally symmetric vibrational mode, the transition from the zero vibrational level of the ground

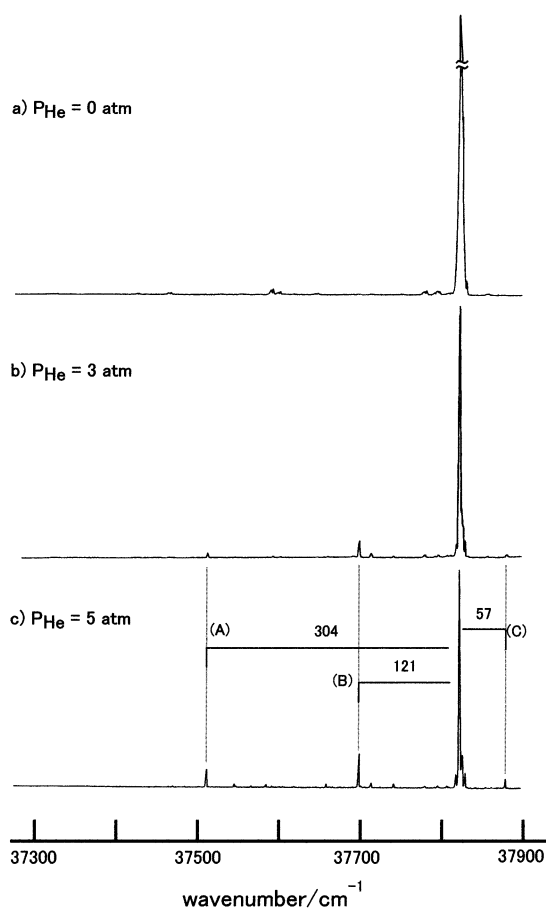


**Figure 4.** Fluorescence excitation spectra of DFP with water at different He pressures.

state to the overtone level in the  $S_1$  state becomes allowed because of the Franck–Condon principle. In this case, the vibronic structure in the electronic spectrum involves non-totally symmetric vibrations that are related to the structural change caused by the electronic transition. For DFP, the appearance of totally symmetric vibrations supports the assignment that the  $S_1$  state is a  ${}^1B_2(\pi, \pi^*)$  state, which is an allowed transition from the  $S_0$  state.

**3.3. Fluorescence Excitation Spectra of Hydrogen-Bonded 2,6-Difluoropyridine–Water Clusters.** Figure 4 shows the spectral change around the electronic origin of bare DFP along with a different pressure of He under the existence of water. Three peaks at  $-304$ ,  $-121$ , and  $+57 \text{ cm}^{-1}$  from the electronic origin of bare DFP clearly appear with increasing He pressure. These bands are due to hydrogen-bonded clusters between DFP and water. The bands are temporarily mentioned as the bands



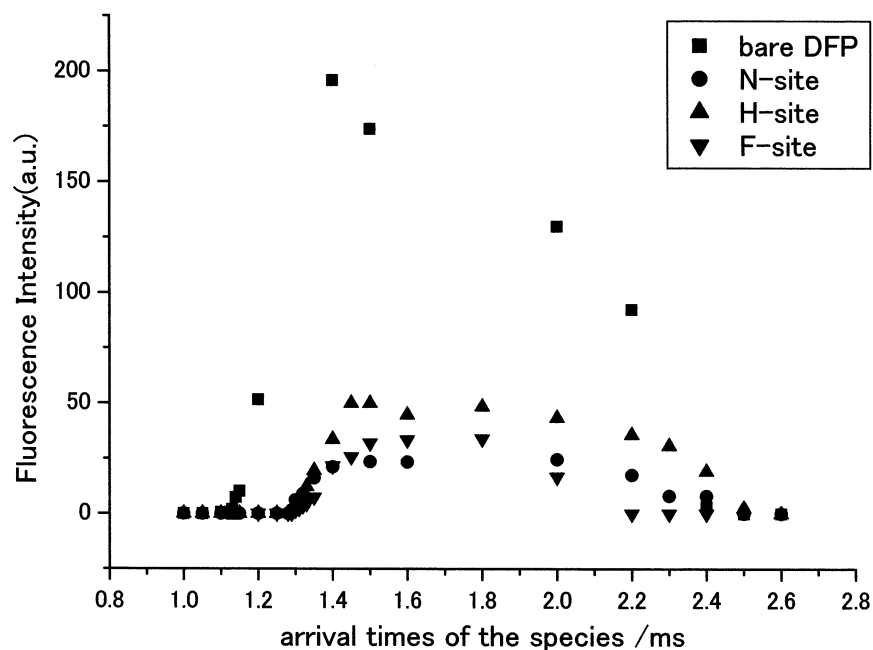


**Figure 5.** Arrival times of the species. The fluorescence intensities of the species were observed with respect to the delay times of the exciting laser from the nozzle opening.

A, B, and C for the bands from lower to higher energy, respectively. If these bands are due to different sizes of clusters, such as 1:2 and/or 1:3, the relative intensity of the bands should change depending on the nozzle condition. However, as can be seen from the Figure, the relative intensities among A, B, and C are unchanged despite the different carrier gas pressure and the concentration of water in the jet. Therefore, these bands are assigned to the clusters containing one water molecule. To ensure the assignment of cluster size, the arrival time<sup>21</sup> of each band was measured, and the results are shown in Figure 5. The band intensities of clusters A, B, and C rise about 1.3 ms after the nozzle opens, and that of bare DFP, about 1.1 ms after the nozzle opens. It is important to note that the arrival times of clusters A, B, and C coincide very well. The experiment strongly supports the fact that bands A, B, and C are due to a 1:1 cluster between DFP and water.

Figure 6 shows the hole-burning spectra with a probe laser tuned to the bands due to each cluster. The intensity of the pump laser was too strong to obtain precise relative intensities in the spectra. As seen from Figure 6, peaks A, B, and C originate from different cluster species. The clusters that give bands A, B, and C are hereafter tentatively called clusters A, B, and C, respectively. With the introduction of D<sub>2</sub>O into the nozzle instead of H<sub>2</sub>O, the three peaks due to the D<sub>2</sub>O clusters shift from those of the DFP–H<sub>2</sub>O clusters, and the results clearly show that the three clusters contain water molecules. As a result of the experiment mentioned above, there exist three cluster species for the DFP–water 1:1 cluster. The band origins of DFP–D<sub>2</sub>O clusters give –2, –2, and +8 cm<sup>–1</sup> shifts from those of A, B, and C of DFP–H<sub>2</sub>O clusters, respectively.

Because both the experiments and the calculations, as mentioned above, show the existence of three isomers for the DFP–water 1:1 cluster, the three clusters observed in the electronic spectra correspond to those obtained in the calculations. Therefore, clusters A, B, and C correspond to three clusters obtained with molecular orbital calculations. Tarakeshwar et al. calculated the stable structures of fluorobenzene–water and *p*-difluorobenzene–water clusters and concluded that the hydrogen of the water molecule bonds to the fluorine atom of the aromatic ring.<sup>11</sup> Brenner et al. also have suggested the

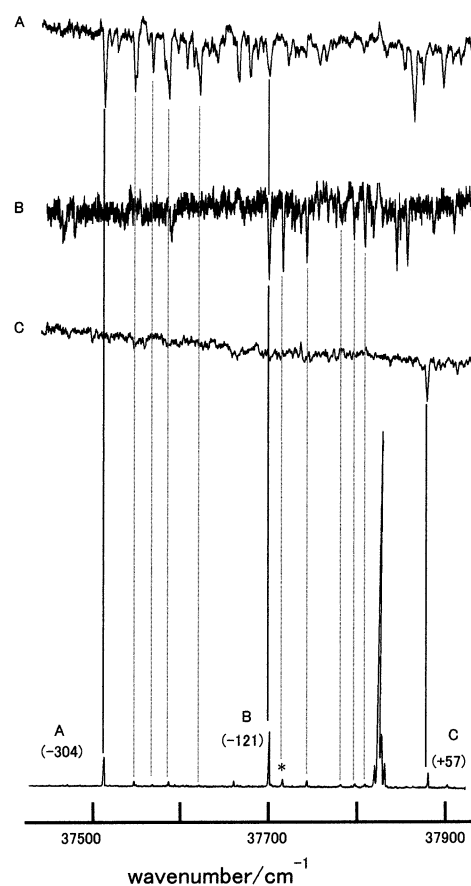


**Figure 6.** Hole-burning spectra of DFP–water clusters (upper three traces) and fluorescence excitation spectrum (lower trace). In the spectra of A and C, bands A and C in the fluorescence excitation spectrum were monitored, respectively. In spectrum B, the band marked with \* was probed because the band due to cluster A coincides with band B. The weak peaks observed around the lower-energy region from the band origin in spectrum B are not reproducible.

existence of a similar structure from the rotational analysis of electronic transitions and theoretical calculations. The structure

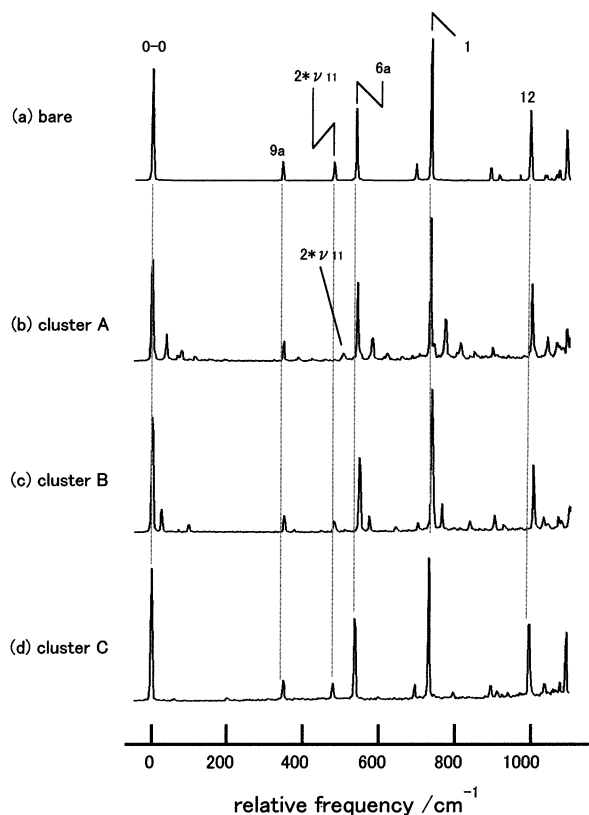


**Figure 7.** SVL spectra from the band origin of (a) bare, (b) cluster A, (c) cluster B, and (d) cluster C.

corresponds to that of the F-site cluster in the DFP–water cluster. The electronic origins of fluorobenzene–water<sup>22</sup> and *p*-difluorobenzene–water<sup>10</sup> clusters appear +117 cm<sup>-1</sup> and +169 cm<sup>-1</sup> higher than those of the bare molecule, respectively. The band origin of cluster C appears +57 cm<sup>-1</sup> higher than that of bare DFP. These shifts suggest that cluster C could be assigned to the F-site cluster as obtained for fluorobenzene–water and *p*-difluorobenzene–water clusters. The strongest band, cluster B, could be assigned to the N-site or H-site cluster. The small red shift of this type of cluster is also observed for 2-fluoropyridine–water and 3-fluoropyridine–water clusters,<sup>23</sup> where the N-site cluster is considered to be the most stable one. If these assignments are correct, then cluster A is assigned to the H-site cluster. The assignment of clusters A and B is tentative and will also be discussed in later sections.

**3.4. Dispersed Fluorescence Spectra of 2,6-Difluoropyridine–Water Clusters.** Figure 7 shows the single vibronic level (SVL) fluorescence spectra from the electronic origins of three clusters together with that of a bare one for comparison. The vibronic structures for the intramolecular vibrations of the three clusters are similar to that of bare DFP. The fact indicates that intramolecular vibrations of the DFP chromophore in the clusters are not significantly perturbed by water with hydrogen bond formation. The vibrational frequency differences of the intramolecular vibrations between bare and DFP–water clusters are very small and less than 7 cm<sup>-1</sup>, as shown in Table 2. One exception is observed in the spectrum of cluster A, shown in Figure 7b. The band observed at 514 cm<sup>-1</sup> could be assigned to the overtone of the out-of-plane ring-deforming vibration,  $\nu_{11}$ , from its intensity. The frequency of the band in bare DFP is observed at 487 cm<sup>-1</sup> (Figure 7a, Table 2). This fact means that the overtone of  $\nu_{11}$  in cluster A has a 27 cm<sup>-1</sup> higher frequency than that of a bare one. The blue shifts of the vibration for H-site

and F-site clusters are also obtained in the molecular orbital calculations, as can be seen in Table 2. Frequency shifts of intramolecular vibrations due to cluster formation were calculated with the B3LYP/6-311++G\*\* and MP2/6-311++G\*\* methods. The two calculations coincide well for the vibrational frequencies. These calculations predict the relatively larger blue shift for  $2\nu_{11}$  of the H-site and F-site clusters. If cluster C is assigned as the F-site cluster, then cluster A is favorable to be assigned as the H-site cluster from the frequency-shift calculations.

In addition to the intramolecular vibrations originating from the vibrations of DFP itself, several low-frequency vibrations due to intermolecular vibrations between DFP and water were observed. In Table 3, calculated and observed frequencies of intermolecular vibrations are shown. The calculated frequencies are closer regardless of the calculation method. In addition to the intramolecular vibrations of DFP and water, there exist six low-frequency vibrations due to hydrogen bonding. Considered from the frequency shifts between DFP–H<sub>2</sub>O and DFP–D<sub>2</sub>O, these six vibrations are divided into two groups, that is, larger and smaller frequency differences between DFP–H<sub>2</sub>O and DFP–D<sub>2</sub>O, as seen from Table 4. The three vibrations with a relatively smaller shift in DFP–D<sub>2</sub>O are assigned to out-of-plane bending, in-plane bending, and stretching vibrations between DFP and water. Three other vibrations with larger shifts are considered to be rotational motions of the water molecule with respect to DFP.

Figure 8 shows the enlarged spectra of the low-frequency regions of Figure 7 together with the spectra of DFP–D<sub>2</sub>O clusters. The SVL spectrum from the band origin of cluster A (H-site cluster), shown in Figure 8a, contains low-frequency vibrations of 31(30), 40(39), 70(66), 80(79), and 117(116) cm<sup>-1</sup>, where the numbers in parentheses indicate the frequencies of DFP–D<sub>2</sub>O clusters. A band at 40 cm<sup>-1</sup> and its overtone bands form the main progressions in the spectra. The bands for the first and second overtones of the vibration are observed at 80 and 117 cm<sup>-1</sup>, respectively. The frequency of the second overtone of 117 cm<sup>-1</sup> indicates the existence of anharmonicity in the higher quanta along the intermolecular bending vibration. The frequency interval suggests that the H-site cluster has a near-harmonic potential surface along the vibrational mode in the ground state. The three vibrational modes out of six intermolecular vibrations are out-of-plane bending, in-plane bending, and stretching vibrations between water and DFP whose calculated frequencies are 31, 24, and 84 cm<sup>-1</sup>, respectively for H-site clusters with the B3LYP/6-311G\*\* calculation. In the H-site cluster, because the oxygen atom lies on the DFP molecular plane, the symmetry of the cluster is *C<sub>s</sub>*. Under *C<sub>s</sub>* symmetry, in-plane bending and stretching vibrations belong to the totally symmetric vibration. Considered from the frequency of the band at 40 cm<sup>-1</sup>, which appears in the SVL spectrum of the H-site cluster, this band could be assigned to an in-plane bending or out-of-plane bending vibration of the hydrogen bond from molecular orbital calculations. In the case of nontotally symmetric vibrations, the longer progression originates from the structural distortion along a symmetry-breaking vibrational mode. The distortion results in the progression of an overtone of a nontotally symmetric vibration-related vibrational mode of the distortion, as observed for 1,2,4,5-tetrafluorobenzene.<sup>24</sup> However, the stronger band origin observed in the electronic spectra removes the possibility of the distortion. Therefore, the band at 40 cm<sup>-1</sup> in the dispersed fluorescence spectrum could be assigned to be a totally symmetric in-plane bending vibration of hydrogen bonding.

**TABLE 3: Frequency Dependence of the Intermolecular Vibrations of DFP–Water Clusters on the Calculation Methods and Basis Sets Together with Observed Frequencies<sup>a</sup>**

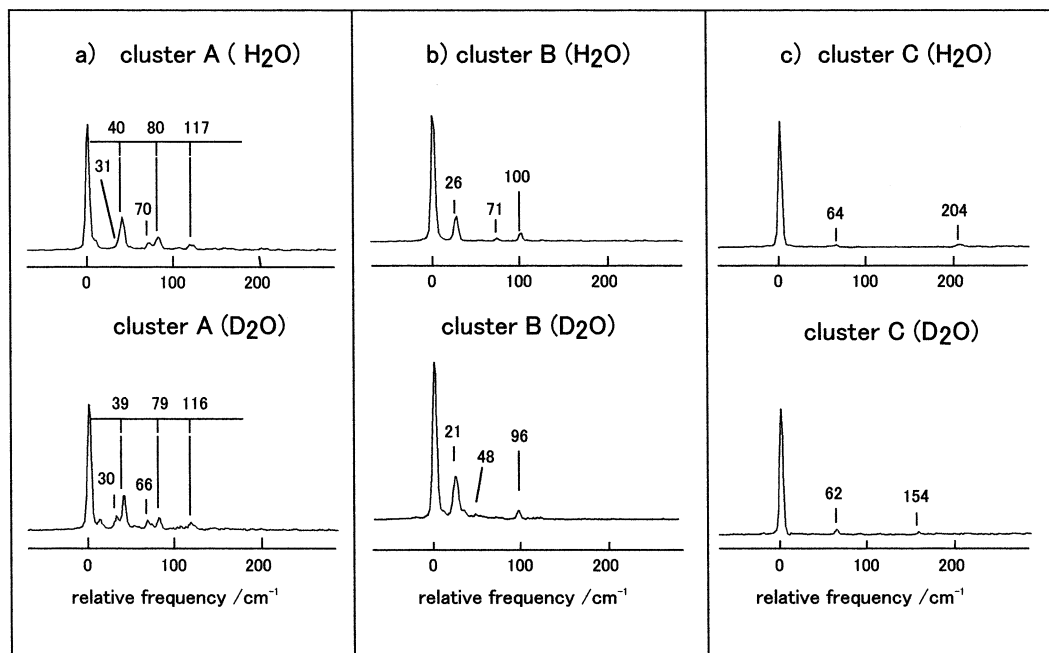
assignment	H-site (A)				obsd	N-site (B)				obsd	F-site (C)				obsd
	MP2		B3LYP			MP2		B3LYP			MP2		B3LYP		
	31G <sup>e</sup>	311G <sup>f</sup>	31G <sup>e</sup>	311G <sup>f</sup>		31G <sup>e</sup>	311G <sup>f</sup>	31G <sup>e</sup>	311G <sup>f</sup>		31G <sup>e</sup>	311G <sup>e</sup>	31G <sup>e</sup>	311G <sup>f</sup>	
$\nu_{\gamma}^b$	31	36	33	31	31	12	8	16	18		32	28	36	30	
$\nu_{\beta}^c$	43	43	34	24	40	53	23	45	33	26	93	76	91	70	64
$\nu_{\alpha}^d$	100	100	94	84	70	123	114	122	109	100	124	112	124	102	
H <sub>2</sub> O rotation	139	135	160	107		161	91	143	102	71	177	180	188	118	
	131	179	115	170		203	276	223	290		195	228	201	233	204
	118	226	104	179		409	455	399	499		435	280	447	297	

<sup>a</sup> All calculated frequencies were obtained without scaling factor correction. <sup>b</sup> Out-of-plane bending vibration. <sup>c</sup> In-plane bending vibration. <sup>d</sup> Stretching vibration. <sup>e</sup> 6-31G\*\* basis set. <sup>f</sup> 6-311++G\*\* basis set.

**TABLE 4: Observed and Calculated Intermolecular Vibrations of DFP–H<sub>2</sub>O and DFP–D<sub>2</sub>O Clusters<sup>a</sup>**

assignment	H-site				N-site				F-site			
	calcd		obsd		calcd		obsd		calcd		obsd	
	H <sub>2</sub> O	D <sub>2</sub> O	H <sub>2</sub> O	D <sub>2</sub> O	H <sub>2</sub> O	D <sub>2</sub> O	H <sub>2</sub> O	D <sub>2</sub> O	H <sub>2</sub> O	D <sub>2</sub> O	H <sub>2</sub> O	D <sub>2</sub> O
$\nu_{\gamma}^b$	31	29	31	30	18	18			30	30		
$\nu_{\beta}^c$	24	23	40	39	33	32	26	21	70	67	64	62
$\nu_{\alpha}^d$	84	80	70	66	109	105	100	96	102	102		
H <sub>2</sub> O rotation	107	76			102	73	71	48	118	84		
	170	131			290	208			233	167	204	154
	179	136			499	349			297	205		

<sup>a</sup> Calculations were made with B3LYP/6-311++G\*\*. <sup>b</sup> Refer to the notation in Table 3.

**Figure 8.** Expanded SVL spectra around the intermolecular vibrational region of the clusters. The upper trace and lower trace are due to DFP–H<sub>2</sub>O and DFP–D<sub>2</sub>O clusters, respectively.

In the dispersed fluorescence spectrum from the band origin of phenol–H<sub>2</sub>O, the intermolecular stretching vibration was observed to be the main progression.<sup>25</sup> The red shift of the electronic origin of cluster A means that the hydrogen bond energy in the excited state is larger than that in the ground state by 304 cm<sup>-1</sup>. Therefore, it is expected that the bond distance between water and DFP in the excited state becomes shorter than that in the ground state. From the Franck–Condon principle, the change in the hydrogen bond distance results in the appearance of a stretching vibration between DFP and water in the electronic spectrum. As a result, the stretching vibration is expected to appear in the electronic spectrum for the cluster

with a large frequency shift of the electronic origin. Therefore, a band at 70 cm<sup>-1</sup> is assigned to a stretching vibration of the hydrogen bond. A band at 31 cm<sup>-1</sup> is weakly observed as a shoulder beside the band at 40 cm<sup>-1</sup> in the spectrum with higher resolution. The band at 30 cm<sup>-1</sup> in the DFP–H<sub>2</sub>O cluster could be assigned as the out-of-plane vibration of the hydrogen bond. These assignments also well explain the deuterium effect of the cluster (i.e., the frequency change of DFP–D<sub>2</sub>O (Table 4)).

The dispersed fluorescence spectrum of cluster B (N-site cluster) gives the bands at 26(21), 71(48), and 100(96) cm<sup>-1</sup> for DFP–H<sub>2</sub>O(DFP–D<sub>2</sub>O). From the consideration of the frequencies and deuterium effects of the cluster, 100- and 71-

$\text{cm}^{-1}$  vibrations are assigned to the stretching and rotational vibrations, respectively. The band at  $26 \text{ cm}^{-1}$  could be assigned to an in-plane or an out-of-plane bending vibration of hydrogen bonding. The stable structure of the N-site cluster is expected to have a nearly planar form as a result of molecular orbital calculations. If the symmetry of the cluster could be treated as  $C_s$ , then the in-plane and out-of-plane vibrations belong to totally and nontotally symmetric vibrations, respectively. As discussed in the H-site cluster, a totally symmetric in-plane bending vibration is suitable as the assignment of the vibration considered from a relatively smaller structural change. Although the intensity of the band is similar to that of the band of the in-plane bending vibration, which appears at  $40 \text{ cm}^{-1}$  for the H-site cluster, the intensity of the overtone band is very weak in the spectrum of the N-site cluster. The band intensity of the totally symmetric vibration is governed by the displacement of the potential minimum, frequency difference, and vibrational mode mixing (Duschinskii effect) between the electronic states. Therefore, the inconsistency in the intensity distribution of the bands between H-site and N-site clusters is due to the difference in the factors mentioned above.

In the spectra of cluster C (Figure 8c), bands at  $64(62)$  and  $204(154) \text{ cm}^{-1}$  due to intermolecular vibrations of DFP– $\text{H}_2\text{O}$  (DFP– $\text{D}_2\text{O}$ ) are observed very weakly. This fact indicates that the displacement of potential minima along the intermolecular vibrational coordinate is very small for the electronic excitation in cluster C. The result well corresponds to the small frequency shift of the band origin from that of bare DFP, which indicates that the strength and stabilization energy of the hydrogen bonding are similar in both states. Although the dispersed fluorescence spectrum of the hydrogen bond cluster usually gives the stretching vibration of the hydrogen bonding, the frequencies of  $64(62)$  and  $204(154) \text{ cm}^{-1}$  are too low and too high, respectively, to be assigned to the stretching vibrations of hydrogen bonding. From the results of molecular orbital calculations, the frequency shifts for DFP– $\text{D}_2\text{O}$  clusters are smaller for bending and stretching vibrations and larger for rotational vibrations in intermolecular vibrations when the  $\text{H}_2\text{O}$  molecule is replaced by  $\text{D}_2\text{O}$  in the DFP–water clusters. Therefore, the bands at  $64$  and  $204 \text{ cm}^{-1}$  are assigned to be an in-plane or an out-of-plane bending vibration or rotational vibration, respectively. From the calculated frequencies, the assignments of the bands are shown in the Table 4. The experimental frequency shifts of DFP– $\text{D}_2\text{O}$  agree well with the molecular orbital calculations. The intermolecular vibration is observed very weakly in the electronic spectrum that is also obtained for *p*-difluorobenzene–water clusters,<sup>25</sup> where the cluster structure corresponds to that of an F-site cluster of DFP–water. The frequency shifts and the features of the electronic transitions also support our structural assignment for DFP–water clusters.

The vibronic structure in the dispersed fluorescence spectra for the three clusters differs in the intensity distribution of the intermolecular vibrations. These results correspond well to the fact that bands A, B, and C originate from different cluster species. In phenol–water clusters, the frequency of the hydrogen-bond stretching vibration is  $155 \text{ cm}^{-1}$  in the electronic ground state.<sup>26</sup> Since the hydrogen bond interaction between DFP and water is weaker than that of phenol–water, the frequency of the hydrogen bond stretching vibration of DFP–water clusters is expected to be lower than that of phenol–water. From the consideration of the stretching frequencies of hydrogen bond vibrations in clusters A and B, it is expected that the strength of the hydrogen bond between DFP and water is smaller than

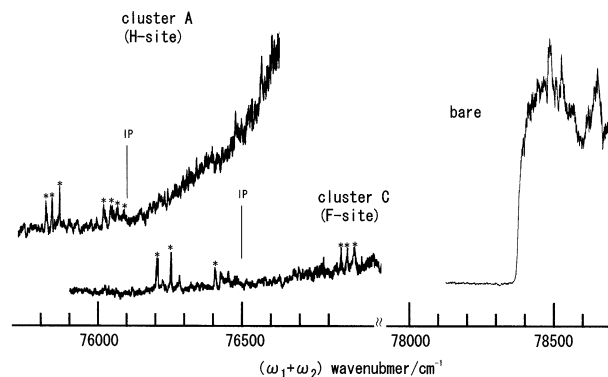


**Figure 9.** Two-color ion yield spectra due to  $(1 + 1')$  REMPI. The energy scale represents the total energy of the excitation (fixed) and ionization (scanned) lasers. The bands marked with \* in the spectra of clusters A and C are due to the one-color REMPI signals from the ionization laser ( $\omega_2$ ) itself.

that of phenol–water clusters. Because the stretching frequency of hydrogen bonding reflects the strength of hydrogen bonding, cluster B has stronger hydrogen bond than cluster A in the ground state, and the molecular orbital calculation also supports this result. The stretching frequency of the F-site cluster was not observed; however, the correspondence between calculated and experimental values is quite good. These facts indicate that the B3LYP/6-311++G\*\* calculation explains the hydrogen bond strength of the DFP–water system, though DFT calculations with the B3LYP functional cannot take into account the dispersion force adequately.<sup>11</sup> In other words, the dispersion force might not be dominant in determining the structure and bond strength of DFP–water clusters.

**3.5. Multiphoton Ionization Spectra of DFP–Water Clusters.** Figure 9 shows the mass-selected ion yield spectra where the ionization laser was scanned to ionize from the  $S_1$  origins of bare cluster A (H-site) and cluster C (F-site), respectively. The ionization potentials of the bare DFP and H-site clusters are determined to be  $78\,375$  and about  $76\,100 \text{ cm}^{-1}$ , respectively. For the F-site cluster, the ionization threshold is too broad to determine the ionization potential precisely; however, the ionization threshold exists around  $76\,500 \text{ cm}^{-1}$ . Because the excitation and ionization laser intensities during the observations for H- and F-site clusters were kept constant, different ionization thresholds between H-site and F-site clusters were ascribed to the difference in the Franck–Condon overlap between the zero vibrational levels of the  $S_1$  and  $D_0$  states in the clusters. A sharp ionization threshold corresponds to a larger Franck–Condon overlap, which indicates a smaller structural change between the  $S_1$  and  $D_0$  states. The H-site cluster gives a relatively sharper ionization threshold than the F-site cluster. This fact indicates that the structural change along with the electronic transition from  $S_1$  to  $D_0$  states is smaller in the H-site cluster than that in F-site cluster. Ab initio molecular orbital calculations for  $D_0$  states indicate that the H-site cluster is stable in the  $D_0$  state and that the F-site cluster is not, as mentioned before. If the F-site cluster is unstable in the  $D_0$  state, then the appearance ionization potential must increase compared to that of the H-site cluster, and the ion yield spectrum becomes broader. As a result, it is concluded that the H-site cluster has a stable structure in the  $D_0$  state and the F-site cluster is unstable in the  $D_0$  state, although both the structures are stable in the  $S_0$  and  $S_1$  states. The two stable structures in the  $D_0$  state have been obtained with molecular orbital calculations (i.e., one is a H-site structure obtained for the  $S_0$  state and another is  $\pi$ -site structure where the oxygen atom of the water molecule bonds to the  $\pi$  electrons,



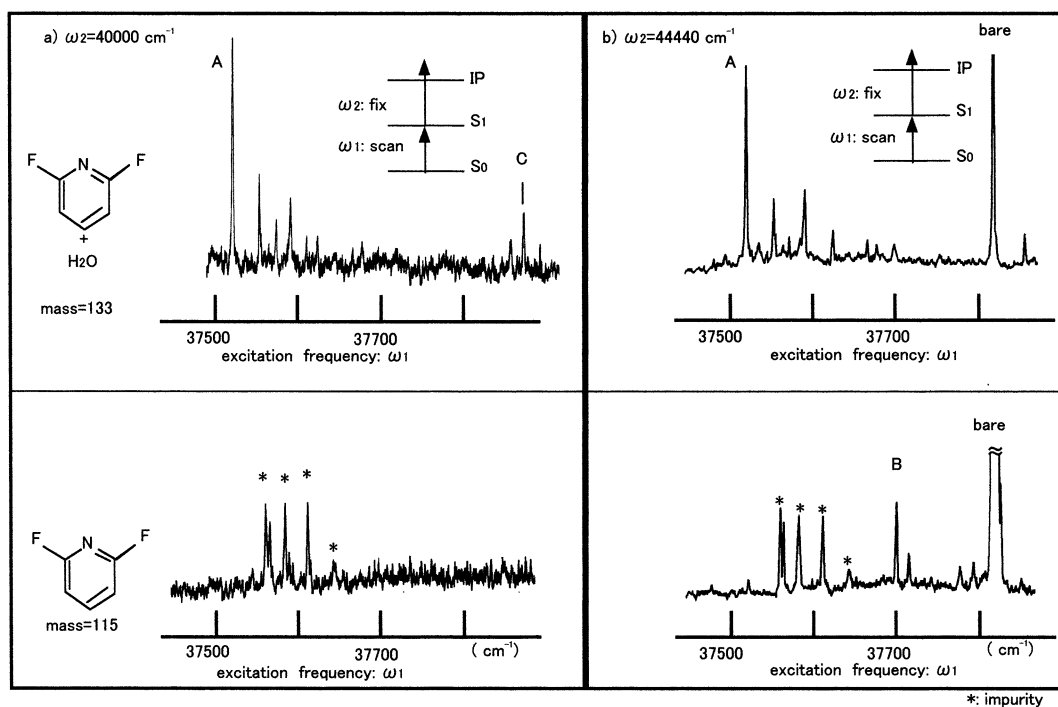


**Figure 10.** Mass-selected two-color ( $1 + 1'$ ) REMPI spectra of DFP–H<sub>2</sub>O clusters. The frequencies of the ionization laser are set to (a) 40 000 and (b) 44 440 cm<sup>-1</sup>. The spectra of the upper traces monitored the mass channel at 133 amu, and the lower, at 115 amu, which correspond to the masses of DFP–H<sub>2</sub>O and bare DFP, respectively.

which is not stable in the  $S_0$  state (Figure 2)). If the structures of the H-site cluster in the  $S_1$  and  $D_0$  states were similar, then the ionization yield spectrum could give a stepwise threshold. However, the ion yield spectrum for the H-site cluster gives a relatively lower threshold. This fact might indicate that the zero vibrational level of the ion could not be accessible from the zero vibrational level in the  $S_1$  state. The B3LYP/6-311++G\*\* calculation of the H-site cluster in the  $S_0$  state shows that the bond length between the oxygen and the ring hydrogen at the  $\gamma$  position, 2.51 Å, is larger than that between the oxygen and the ring hydrogen at the  $\beta$  position, 2.30 Å. (See Figure 1.) However, the above relationship in the  $S_0$  state is reversed in the  $D_0$  state. (See Figure 2.) That is, the bond length between the oxygen and the  $\gamma$  hydrogen is shorter than that between the oxygen and the  $\beta$  hydrogen in the  $D_0$  state. The distance between the oxygen and  $\gamma$  hydrogen is similar both in the  $S_0$  and  $D_0$  states. However, the distance between the oxygen and  $\beta$  hydrogen becomes shorter in the  $D_0$  states by 0.43 Å. From the electronic spectrum of the H-site cluster, the structural change between the  $S_0$  and  $S_1$  states is small because the intensity of the band origin is the strongest among the intermolecular modes. This fact means that the bond distance in the  $S_0$  and  $S_1$  states could be similar. If the B3LYP/6-311++G\*\* calculations predict the hydrogen bond distance correctly, then the geometry change along with ionization might be quite large for H-site clusters. The absence of a stepwise threshold for the ionization yield spectrum regardless of the transition within the corresponding structure between the  $S_1$  and  $D_0$  states might be ascribed to the change in the hydrogen bond distance with the ionization of the H-site cluster.

Figure 10 shows the mass-selected  $S_1$ – $S_0$  excitation spectra, where the two different ionization energies were used for the ionization from  $S_1$  to  $D_0$  states. The ionization energies that are used are 40 000 and 44 440 cm<sup>-1</sup>, and the results are shown in Figures 10a and 9b, respectively. As can be seen in Figure 10a, the energy of 40 000 cm<sup>-1</sup> can ionize the H-site and F-site clusters but cannot ionize bare DFP. As expected from the

ionization energy of H-site and F-site clusters, the bands due to H-site and F-site clusters were observed in the spectra at the mass channel of 133 amu. The absence of the N-site cluster in the spectra indicates the increase in the ionization energy for the N-site cluster. The energy of 44 440 cm<sup>-1</sup> for the ionization laser can ionize the N-site cluster, and it gives the bands at the mass channel of 115 that corresponds to the mass number of bare DFP, as shown in Figure 10b. The ionization laser was scanned in this region; however, the ionization threshold is too broad to determine the clear ionization onset. Therefore, the ionization threshold was determined by observing the appearance of the origin band of the N-site cluster with various fixed ionization lasers in the ( $1 + 1'$ ) REMPI spectra. The appearance energy of the band due to the N-site cluster was determined to exist between 79 240 and 80 190 cm<sup>-1</sup>. A weak band observed at the mass channel of 133 in Figure 10b, which is close to the electronic origin of cluster B, is assigned to a band due to cluster A from the result of the hole-burning spectrum shown in Figure 6. This fact means that the N-site cluster is ionized with a frequency of 44 440 cm<sup>-1</sup> from the zero vibrational level of the  $S_1$  state and dissociates after the ionization. Therefore, the total energy of 81 956 cm<sup>-1</sup> exceeds the dissociation limit of the N-site cluster cation. The ab initio calculations also indicate that the N-site cluster is not stable in the  $D_0$  state, although the structure is most stable among the three isomers in the  $S_0$  state. The calculation also shows that the H-site cluster is the only stable structure among the three stable structures in the  $S_0$  state. As shown in Figure 9, the photoionization spectra of the H-site cluster give sharper ionization thresholds than the spectra of the F-site cluster. This phenomenon coincides with the stability of the H-site cluster in  $S_0$  and  $D_0$  states as obtained in the molecular orbital calculation. The broad threshold of the F-site and N-site clusters might be due to the unstable structure in the  $D_0$  state as obtained in the molecular orbital calculation. The ab initio molecular orbital calculation with the method of B3LYP/6-311++G\*\* well supports the experimental results for the  $S_0$  and  $D_0$  states of DFP–water clusters.

#### 4. Conclusions

The electronic spectra of DFP with water in a supersonic free jet were observed, and the spectra showed the existence of three structural isomers for DFP–water 1:1 clusters. The structures of the clusters are as follows.

(1) H-site cluster: The oxygen atom of water bonds to two hydrogen atoms at the 3,4 positions of DFP. The strength of the hydrogen bonding is stronger in the  $S_1$  state than in the  $S_0$  state. The cluster is also stable in the  $D_0$  state.

(2) N-site cluster: The structure of the cluster is to be expected for aza-aromatic molecules such as pyridine, which has a proton-accepting site through the lone-pair electrons on the nitrogen atom in the aromatic ring. From the calculations of MP2/6-311++G\*\* and B3LYP/6-311++G\*\*, the hydrogen bonding energy is highest among the three clusters. The cluster has a higher appearance ionization energy than the bare molecule and dissociates after photoionization from multiphoton ionization experiments. The ab initio molecular orbital calculation also supports this result. This fact indicates that the hydrogen bonding of water to nitrogen increases the vertical ionization potential of DFP. This fact is in marked contrast to the results of phenol–water clusters, where the ionization potential of the cluster substantially decreases.<sup>27</sup>

(3) F-site cluster: This type of structure was also observed for *p*-difluorobenzene–water clusters. The cluster is not stable in the  $D_0$  state. The ab initio molecular orbital calculation also supports the instability of the clusters in the  $D_0$  state.

The ab initio molecular orbital calculation with B3LYP/6-311++G\*\* well supports the experimental results obtained for DFP–water clusters in  $S_0$  and  $D_0$  states. The existence of the three structural isomers in DFP–water clusters is due to the similar stabilization energy of the 1:1 clusters in the  $S_0$  state.

#### References and Notes

- (1) Villa, E.; Amirav, A.; Lim, E. C. *J. Phys. Chem.* **1988**, *92*, 5393.
- (2) Becucci, M.; Lakin, N. M.; Pietraprazia, G.; Salvi, P. R.; Castellucci, E.; Kerstel, E. R. Th. *J. Chem. Phys.* **1997**, *107*, 10399.
- (3) Hager, J.; Wallace, S. C. *J. Phys. Chem.* **1985**, *89*, 3833.
- (4) For example, Kryachko, E. S.; Nakatsuji, H. *J. Phys. Chem. A* **2002**, *106*, 731 and references therein.
- (5) Felker, P. M.; Zewail, A. H. *Chem. Phys. Lett.* **1983**, *94*, 448.
- (6) Felker, P. M.; Zewail, A. H. *Chem. Phys. Lett.* **1983**, *94*, 454.
- (7) Wanna, J.; Bernstein, E. R. *J. Chem. Phys.* **1987**, *86*, 6707.
- (8) Mitsui, M.; Ohshima, Y.; Ishiuchi, S.; Sakai, M.; Fujii, M. *Chem. Phys. Lett.* **2000**, *317*, 211.

(9) Barth, H. D.; Buchhold, K.; Djafari, S.; Reimann, B.; Lommatzsch, U.; Brutschy, B. *Chem. Phys.* **1998**, *239*, 49.

(10) Brenner, V.; Martrenchard-Barra, S.; Millie, P.; Dedonder-Lardeux, C.; Jouvet, C.; Solgadi, D. *J. Phys. Chem.* **1995**, *99*, 5848.

(11) Tarakeshwar, P.; Kim, K. S.; Brutschy, B. *J. Chem. Phys.* **1999**, *110*, 8501.

(12) Frisch, M. J.; Trucks, G. W.; Schlegel, H. B.; Scuseria, G. E.; Robb, M. A.; Cheeseman, J. R.; Zakrzewski, V. G.; Montgomery, J. A., Jr.; Stratmann, R. E.; Burant, J. C.; Dapprich, S.; Millam, J. M.; Daniels, A. D.; Kudin, K. N.; Strain, M. C.; Farkas, O.; Tomasi, J.; Barone, V.; Cossi, M.; Cammi, R.; Mennucci, B.; Pomelli, C.; Adamo, C.; Clifford, S.; Ochterski, J.; Petersson, G. A.; Ayala, P. Y.; Cui, Q.; Morokuma, K.; Malick, D. K.; Rabuck, A. D.; Raghavachari, K.; Foresman, J. B.; Cioslowski, J.; Ortiz, J. V.; Stefanov, B. B.; Liu, G.; Liashenko, A.; Piskorz, P.; Komaromi, I.; Gomperts, R.; Martin, R. L.; Fox, D. J.; Keith, T.; Al-Laham, M. A.; Peng, C. Y.; Nanayakkara, A.; Gonzalez, C.; Challacombe, M.; Gill, P. M. W.; Johnson, B. G.; Chen, W.; Wong, M. W.; Andres, J. L.; Head-Gordon, M.; Replogle, E. S.; Pople, J. A. *Gaussian 98*, revision A.9; Gaussian, Inc.: Pittsburgh, PA, 1998.

(13) (a) Kim, K. S.; Lee, J. Y.; Choi, H. S.; Kim, J.; Jang, J. H. *Chem. Phys. Lett.* **1997**, *265*, 497. (b) Courty, A.; Mons, M.; Dimicoli, I.; Piuze, F.; Gaigeot, M. P.; Brenner, V.; Pujol, P.; Mille, P. *J. Chem. Phys. A* **1998**, *102*, 6590. (c) Tachikawa, H.; Igarashi, M. *J. Phys. Chem. A* **1998**, *102*, 8648.

(14) (a) Dkhissi, A.; Adamowicz, L.; Maes, G. *J. Phys. Chem. A* **2000**, *104*, 2112. (b) Papai, I.; Jancso, G. *J. Phys. Chem. A* **2000**, *104*, 2132. (c) Schlucker, A.; Singh, R. K.; Asthana, B. P.; Popp, J.; Kieferr, W. *J. Phys. Chem. A* **2001**, *105*, 1983.

(15) Boys, S. F.; Bernardi, F. *Mol. Phys.* **1970**, *19*, 553.

(16) Nibu, Y.; Sakamoto, D.; Satoh, T.; Shimada, H. *Chem. Phys. Lett.* **1996**, *262*, 615.

(17) (a) Medhi, K. C. *Indian J. Phys., B* **1987**, *61*, 62. (b) Medhi, K. C.; Medhi, R. N. *Spectrochimica Acta, Part A* **1990**, *46*, 1169. (c) Medhi, K. C. *Spectrochimica Acta, Part A* **1986**, *42*, 1393. (d) Medhi, K. C.; Medhi, R. N. *Spectrochimica Acta, Part A* **1990**, *46*, 1333.

(18) Bondybey, V. E.; English, J. H.; Shiley, R. H. *J. Chem. Phys.* **1982**, *77*, 4826.

(19) (a) Bailey, R. T.; Steele, D. *Spectrochimica Acta, Part A* **1967**, *23*, 2997. (b) Green, J. H. S.; Harrison D. J.; Kipps, M. R. *Spectrochimica Acta, Part A* **1973**, *29*, 1177. (c) Lui, S.; Suzuki, S.; Ladd, J. A. *Spectrochimica Acta, Part A* **1978**, *34*, 583.

(20) Wilson, E. B.; Decius, J. C.; Cross, P. C. *Molecular Vibrations*; Dover: New York, 1980.

(21) Li, S.; Bernstein, E. R. *J. Chem. Phys.* **1992**, *97*, 804.

(22) Maeyama, T.; Mikami, N. *J. Phys. Chem.* **1991**, *95*, 7197.

(23) Okabe, C.; Ohsaki, T.; Miyawaki, H.; Nibu, Y.; Shimada, H. To be submitted for publication.

(24) Okuyama, K.; Kakinuma, T.; Fujii, M.; Mikami, N.; Ito, M. *J. Phys. Chem.* **1986**, *90*, 3948.

(25) Tsukamoto, K.; Nibu, Y.; Shimada, H. To be submitted for publication.

(26) (a) Abe, H.; Mikami, N.; Ito, M.; Udagawa, Y. *J. Phys. Chem.* **1982**, *86*, 2567. (b) Schütz, M.; Bürgi, T.; Leutwyler, S. *J. Chem. Phys.* **1993**, *98*, 3763.

(27) Dopfer, O.; Müller-Dethlefs, K. *J. Chem. Phys.* **1994**, *101*, 8508.